ACS OMEGA

http://pubs.acs.org/journal/acsodf

Article

Rheological Impact of Particle Size Gradation on GAP Propellant Slurries

Yi Wang,* Yana Wang, Xiaolan Song,* Chongwei An, and Fengsheng Li

Cite This: *ACS Omega* 2022, 7, 38536−38542

Read Online

ACCESS | Metrics & More | Article Recommendations

ABSTRACT: Over the years, widespread interest has been placed on rheological properties to reflect the processability of propellant slurries. Particle gradation technology plays an essential role in the improvement of the processability of propellant slurries. In this article, rheological properties of glycidyl azide polymer (GAP) propellant slurries were measured by dynamic rheological measurements with a rheometer. Submicron-sized (d_{50} = 0.221 μm) and micron-sized (d_{50} = 33.02 μm) CL-20 particles and ultrafine (d_{50} = 2.40 μm) and micron-sized (d_{50} = 341.69 μm) AP particles were utilized to investigate the influence of the addition of CL-20 and particle size gradation on rheological properties. The test results demonstrate that the LVE region remains almost invariable while the yield transition process is delayed when the relative content of submicron-sized CL-20 increases from 10 to 20%. The values of G', G'', and $|\eta^*|$ increase with increasing submicron-sized CL-20. Despite this, the value of $|\eta^*|$ can be effectively reduced to about the same value as the slurries with bimodal AP by the size gradation of CL-20. In addition, particle porosity appears to be a suitable parameter to predict trends concerning the rheological properties of the GAP propellant slurries.

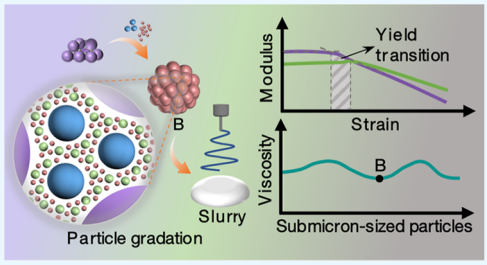

1. INTRODUCTION

Methods to overcome the high energy and low mechanical sensitivity of solid propellants have become a research hotspot by academicians. 2,4,6,8,10,12-Hexanitro-2,4,6,8,10,12-hexaazaisowurtzitane in the ε form (ε-CL-20) has a caged skeleton with high tension and the energetic groups -N-NO_2 and, therefore, is regarded as a powerful oxidizer in solid propellant formulations to entail enhanced energy.[1,2] Unfortunately, growing concerns arise when it comes to the inferior sensitivity of ε-CL-20 to impact, friction, and electric sparks, which causes high-probability hazards during the operation and constrains its extensive application. The addition of glycidyl azide polymer (GAP) is reliable in breaking through the restriction on account of the excellent insensitivity of GAP confirmed by Yanju et al.,[3] Hussein et al.,[4] and Song et al.[5] However, the poor flexibility in the backbone of GAP poses a threat to the desired mechanical properties for solid propellants.[6] Although the plasticizer nitroglycerin (NG) possesses a high density, high energy, and positive oxygen balance, the high sensibility and freezing point (13.2 °C) preclude it from meeting the demand for improved mechanical properties of GAP-based propellants, especially at a low temperature. Diglycerol tetranitrate (DGTN) is a kind of nitrate ester plasticizer with energy characteristics analogous to NG, such as a density of 1.522 g·cm^{-3}, detonation velocity of 7.80 km·s^{-1}, and detonation heat of 6003.4 kJ·kg^{-1}.[7] Meanwhile, its lower values of freezing point (<100 °C) and mechanical insensibility and similar values of solubility parameter to GAP (21.7 MPa$^{0.5}$) represent an effective improvement in the operational safety and mechanical properties of GAP-based propellants as far as the propellant formulation is concerned.[7,8]

In addition to the optimized propellant formulation, the robust performance of solid propellants requires excellent processability of uncured propellant slurries. Otherwise, defects such as voids, shrinkage, and cracks will occur inside the propellant column, which severely defeats the original purpose of developing a solid propellant with high energy and low sensitivity. In response to these challenges, rheological tests have been introduced, and the rheological behavior of the slurries obtained from the experiments allows us to deduce their processability.[9,10] Propellant slurries are generally seen as a class of soft matter whose rheological behavior differs from that of solids and liquids, exhibiting viscoelasticity when subjected to deformation and flow. Steady rheological tests and dynamic rheological tests are two of the prevalent rheological measurement methods. In terms of the regulation of the rheological properties of propellant slurries, particle gradation, the technology of mixing the particles with different sizes in different percentages, has gained momentum.[11,12] In other

Received: June 21, 2022
Accepted: October 12, 2022
Published: October 20, 2022

https://doi.org/10.1021/acsomega.2c03872
ACS Omega 2022, 7, 38536−38542

Table 1. Materials Utilized for This Work

sample	property	source
GAP	number-average molecular weight of 2000, hydroxyl value of 81.97 mgKOH·g^{-1}	the 42nd Institute of the Fourth Academy of China Aerospace Science and Technology Corporation
DGTN		see our previous work for synthetic details[7]
AP	micron-sized, crystal density of 1.95 g·cm^{-3}, analytically pure	Sinopharm Group chemical reagent Co., Ltd.
	ultrafine, crystal density of 1.95 g·cm^{-3}	mechanical ball-milling of micron-sized AP
ε-CL-20 (hereafter "CL-20")	micron-sized, crystal density of 2.04 g·cm^{-3}, analytically pure	Liaoning Qingyang Chemical Industry Company
	submicron-sized, crystal density of 2.04 g·cm^{-3}, analytically pure	Liaoning Qingyang Chemical Industry Company

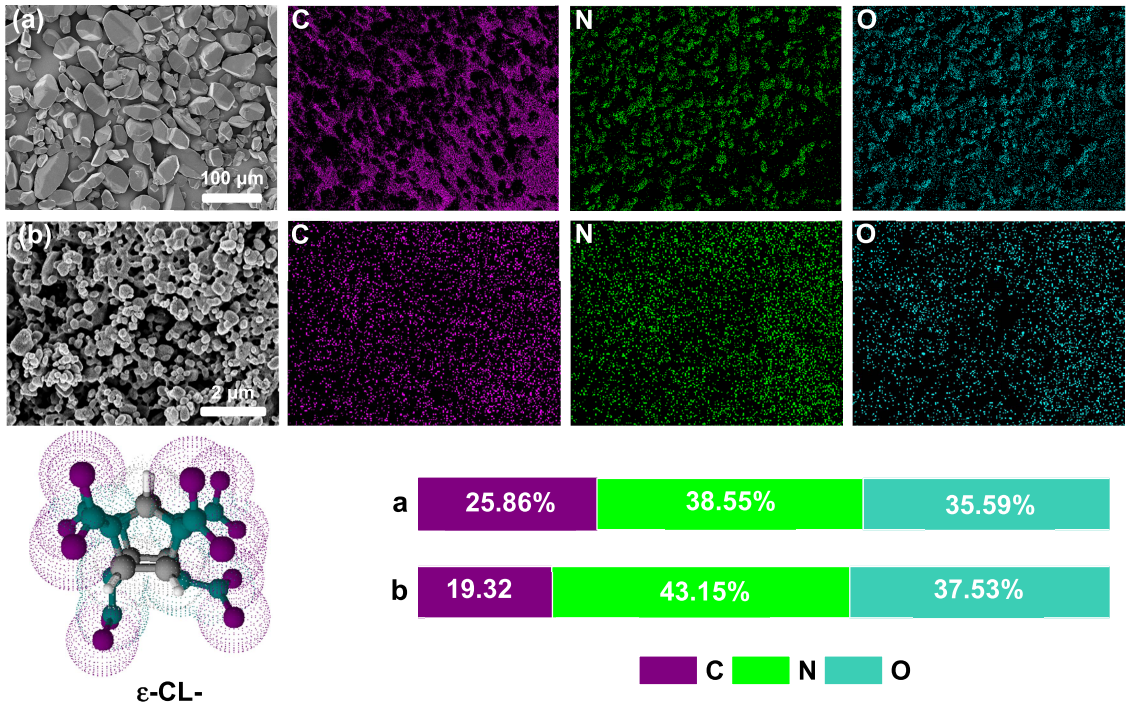

Figure 1. Scanning electron micrographs and elemental distribution of C, N, and O for (a) spindle-shaped and (b) sphere-like CL-20 particles.

words, the size distribution of particles in propellant slurries is altered by particle gradation technology.

In this work, the rheological properties of GAP propellant slurries, wherein GAP acts as a binder, DGTN as an energetic plasticizer, and AP or CL-20 as an oxidizer, were investigated by dynamic rheological measurements. Strain sweep measurements were employed to determine the linear viscoelastic (LVE) region and yield transition of the slurries. Additionally, the influence of particle size and size gradation of AP and CL-20 on the rheological properties of the slurries was revealed by frequency sweep measurements.

2. EXPERIMENTAL SECTION

2.1. Fabrication of the GAP Propellant Slurries. The materials utilized for the fabrication of the GAP propellant slurries are listed in Table 1. Mechanical treatments were performed to obtain samples, including mixing each ingredient and kneading the mixture. GAP and DGTN were mixed first, and subsequently, AP or CL-20 was added to the mixture above in sequence and multiple batches. Before the process, freeze-drying was applied to AP and CL-20 particles. Prompt placement onto the Peltier plate of the rheometer was performed for the resulting GAP propellant slurries after the well-developed kneading. The solid content was identified as 65% based on our previous study on AP/GAP slurries.

2.2. Dynamic Rheological Measurements. A rheometer (Anton Paar MCR102, Graz, Austria) with a 25mm parallel-plate geometry was used for dynamic rheological measurements. First, the measurement temperature was increased to 50 °C, and the sample was not transferred to the Peltier plate until the temperature deviation was less than 0.02 °C. This procedure was adopted when obtaining fresh slurry, as mentioned in the section "Fabrication of the GAP Propellant Slurries." Then, the sample was allowed to stand for 15 min to ensure the same thermal history and the available residual force inside the sample.[12] The Peltier plate was subsequently dropped to a gap of 1mm, which denotes that the upper plate was 1mm away from the lower plate. Finally, strain sweep measurements and frequency sweep measurements were conducted to determine the rheological properties of the samples. When the strain was swept, the strain was altered from 0.0001 to 10% and the angular frequency was set at 10 rad·s^{-1}; based on a constant strain drawn from the linear viscoelastic region of the samples, the angular frequency was changed from 1 to 100 rad·s^{-1} when the frequency was swept. For both, the rheological parameters, including the storage modulus (G'), loss modulus (G''), and complex viscosity ($|\eta^*|$), were documented by Anton Paar RheoCompass software. Each sample was measured three times, and the reproducible results were used for further analysis.

https://doi.org/10.1021/acsomega.2c03872
ACS Omega 2022, 7, 38536−38542

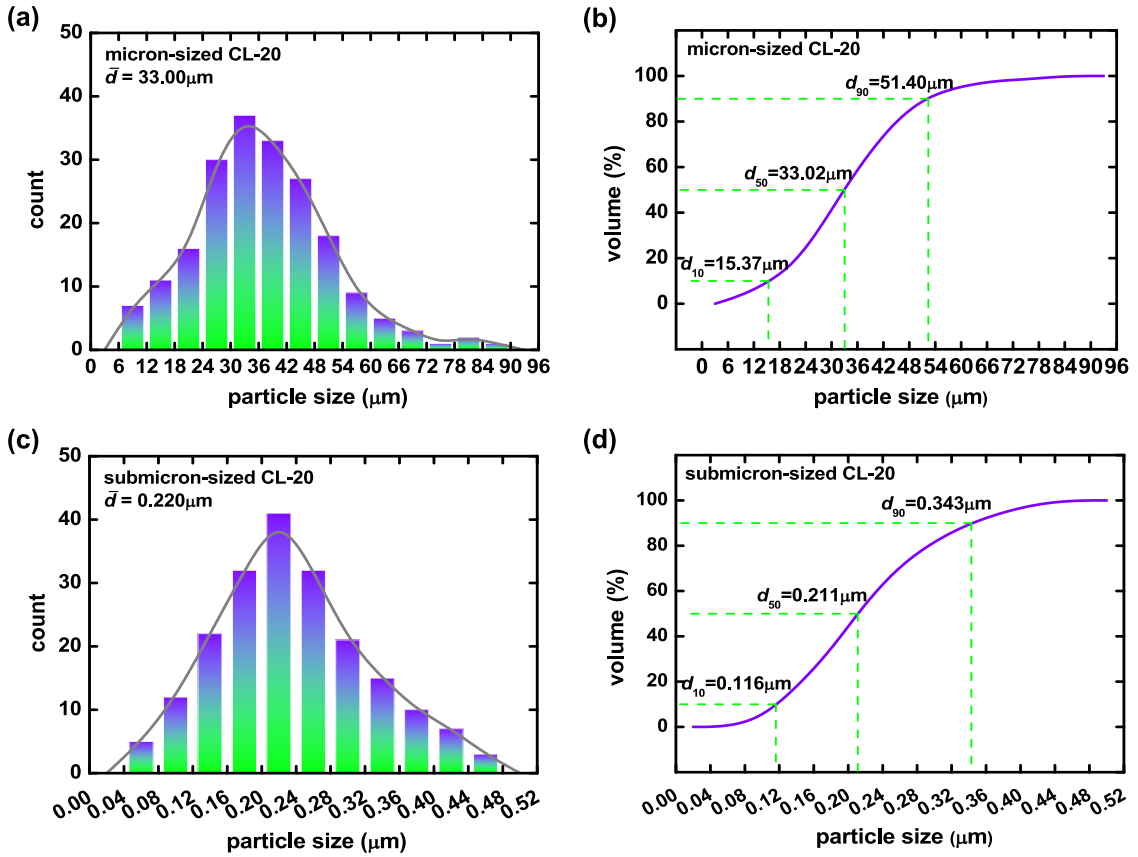

Figure 2. Frequency distribution and cumulative distribution curves of (a, b) micron-sized CL-20 and (c, d) submicron-sized CL-20.

2.3. Scanning Electron Microscopy (SEM). The morphological characteristics of CL-20 particles were observed using a scanning electron microscope (SEM, ZEISS, Germany) at an acceleration voltage of 15kV. The SEM images were handled using IMAGE PRO image processing software to obtain their projection area (S), projection diameter (d), and projection perimeter (C) for the comparison of the sphericity (Φ) and span.

2.4. Brunauer–Emmett–Teller (BET). The specific surface areas of CL-20 particles were determined by the Brunauer–Emmett–Teller (BET) method (Quantachrome Autosorb IQ3, America).

3. RESULTS AND DISCUSSION

3.1. Morphological Characteristics of CL-20. Figure 1 reveals the scanning electron micrographs and elemental distribution of C, N, and O of two types of CL-20. CL-20 particles in Figure 1a carry sharp edges, some of which are spindle-shaped and others are prismatic. Nevertheless, CL-20 particles in Figure 1b are sphere-like in shape with smooth corners and possess smaller particle sizes. This is why refinement is perceived as one of the most prevalent and fundamental strategies to reduce the mechanical sensitivity for CL-20.[5,13,14] Additionally, greater distribution densities of N and O elements, as observed in Figure 1, exist on the surface of CL-20 particles, which signals enhanced energy for finer CL-20. Figure 2 indicates the frequency distribution and cumulative distribution curves for two types of CL-20. The particle sizes are evidently different, one being classified on the micron-grade scale and the other on the submicron-grade scale. The mean diameter ($\bar{d}$) of CL-20 is similar to the median diameter (d_{50}), specifically 33.02 μm for micron-sized CL-20 and 0.221 μm for submicron-sized CL-20. From the values of Φ and span in Table 2, micron-sized CL-20 and submicron-sized CL-20 possess different irregularities and similar polydispersities.

Table 2. Φ, Span, and Specific Surface Area of CL-20[a]

sample	Φ	span	specific surface area ($m^2 \cdot g^{-1}$)
micron-sized CL-20	0.8956	1.091	0.532
submicron-sized CL-20	0.9465	1.076	0.701

[a]Note: $\phi = \frac{4\pi S}{C^2}$, span $= \frac{d_{90} - d_{10}}{d_{50}}$.

Figure 3 presents N_2 sorption isotherms of micron-sized CL-20 and submicron-sized CL-20. The specific surface area, the aggregate of pore surface area, and the external surface area of particles are accessible by the BET method. The adsorption isotherms belong to Type II and the hysteresis loops are Type H3 according to the IUPAC classification.[15−17] An inflection point of the isotherm appears at a low p/p^0, corresponding to the adsorption saturation of the monolayer molecules. When the p/p^0 continues to increase, the adsorption of multilayer molecules begins and capillary coalescence follows, which is confirmed by the presence of a hysteresis loop.[17] Considering the nonporous nature of CL-20, the hysteresis loop may be attributed to the micropores from particle accumulation and aggregates. From Table 2, the specific surface area of 0.701 $m^2 \cdot g^{-1}$ for submicron-sized CL-20 is higher as compared with that of 0.532 $m^2 \cdot g^{-1}$ for micron-sized CL-20, which complies with the fact that the specific surface area of particles is inversely proportional to the particle size. From the above analysis,

https://doi.org/10.1021/acsomega.2c03872
ACS Omega 2022, 7, 38536−38542

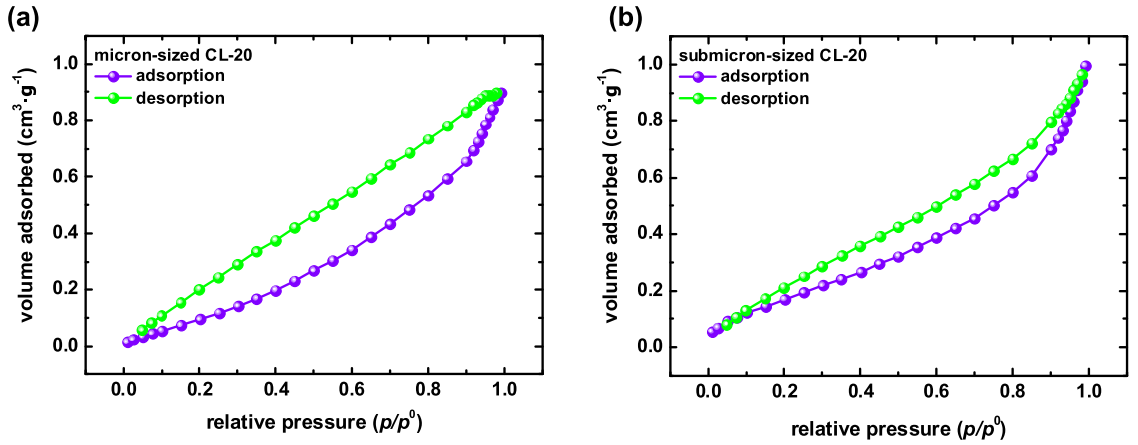

Figure 3. N_2 sorption isotherms of (a) micron-sized CL-20 and (b) submicron-sized CL-20 at 77K.

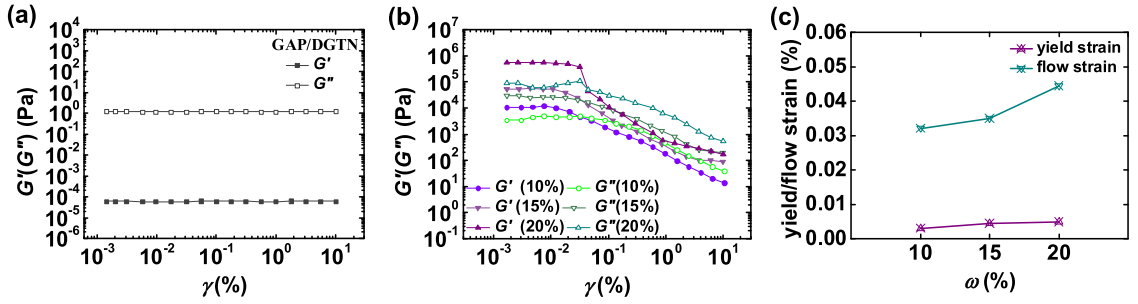

Figure 4. Storage modulus and loss modulus of (a) the GAP/DGTN mixture and (b) the GAP propellant slurries containing different contents of submicron-sized CL-20 at 10 rad·s^{-1} and (c) the yield/flow strains.

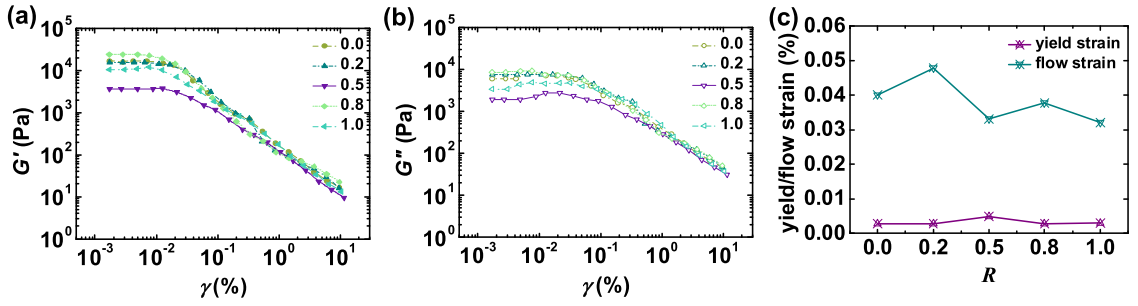

Figure 5. (a) Storage modulus and (b) loss modulus of the GAP propellant slurries with multimodal particles at 10 rad·s^{-1} and (c) the yield/flow strains.

reduced mechanical sensibility, more adequate burning, and different rheological properties could be deduced when micron-sized CL-20 is replaced with submicron-sized CL-20 partially or wholly in the CL-20/AP/GAP propellant slurries.

3.2. Linear Viscoelastic Region of the GAP Propellant Slurries. Strain sweep measurements link rheological properties to the strain response to the internal structure of materials. A GAP/DGTN mixture and GAP propellant slurries containing different contents of submicron-sized CL-20 were tested at 50 °C, and the results are illustrated in Figure 4. Compared with the GAP/DGTN mixture, the rheological behavior of the propellant slurries is significantly distinct. In the linear region, the loss modulus of the GAP/DGTN mixture is greater, which is the opposite in the case of slurries. The moduli of the GAP/DGTN mixture were constant over the test range of strains. Nevertheless, the storage modulus (G') and loss modulus (G'') of the GAP propellant slurries decrease at higher strains, strongly relying on the strain amplitude (Payne effect).[18,19] The critical strain at which the G' begins to drop, which is termed the yield strain of the slurries, reflects the end of the linear viscoelastic (LVE) region and the beginning of the yield transition process. Furthermore, the strain where the value of G' is equal to that of G'' refers to the flow strain of the slurries, which represents the termination of the yield transition process. For the GAP propellant slurries with different contents of submicron-sized CL-20, the yield strain is almost unchanged, and the flow strain increases slightly with increasing submicron-sized CL-20. Both the storage modulus (G') and loss modulus (G'') of the slurries increase with the increase in submicron-sized CL-20. Additionally, the weak strain overshoot behavior could be observed, particularly for the slurries with 20% submicron-sized CL-20.[20,21] In theory, the interfacial tension between GAP and CL-20 of 33.25 mN·m^{-1}[22] renders a greater value as compared with that between GAP and AP of 0.31 mN·m^{-1},[23] demonstrating a stronger solid−liquid interfacial interaction.

https://doi.org/10.1021/acsomega.2c03872
ACS Omega 2022, 7, 38536−38542

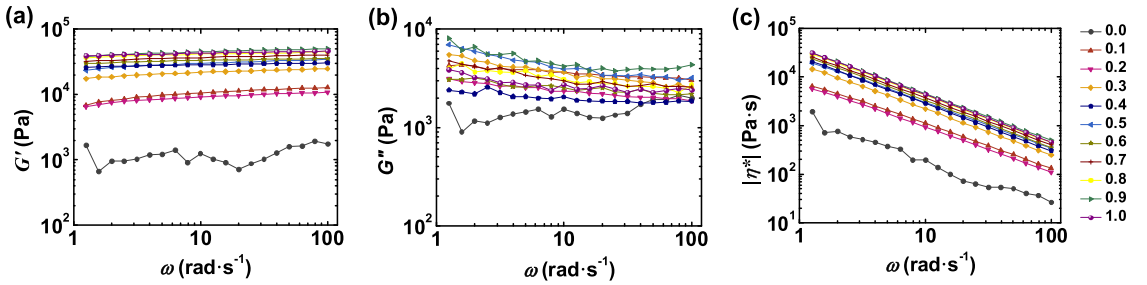

Figure 6. (a) Storage modulus, (b) loss modulus, and (c) complex viscosity of the AP/GAP propellant slurries containing different contents of ultrafine AP.

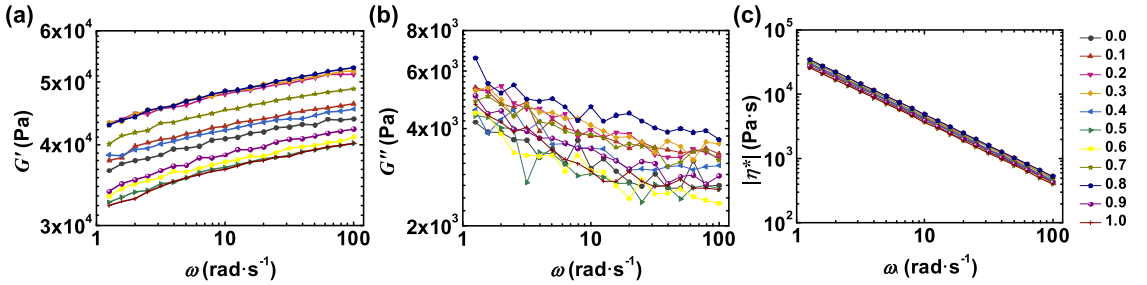

Figure 7. (a) Storage modulus, (b) loss modulus, and (c) complex viscosity of the CL-20/AP/GAP propellant slurries containing different contents of submicron-sized CL-20.

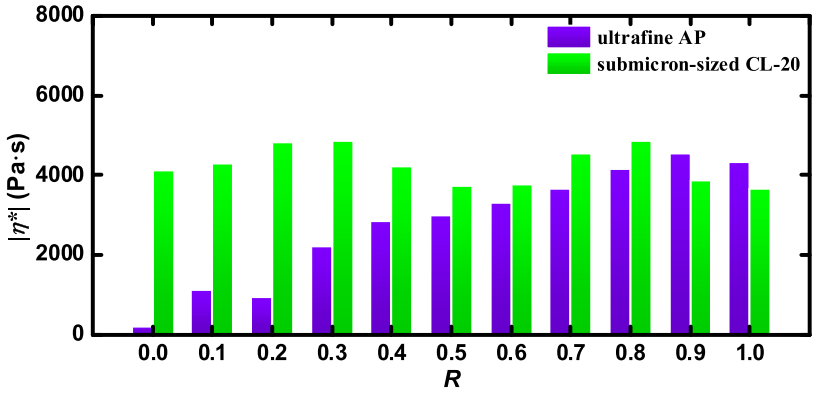

Figure 8. Relationship between the relative content of ultrafine AP and submicron-sized CL-20 and the complex viscosity of the propellant slurries.

The modulus would decrease if AP is replaced by an increasing amount of CL-20, which is incompatible with the foregoing results. The conjecture is that the much smaller particle size of submicron-sized CL-20 than AP, regardless of whether micron-sized AP or ultrafine AP, contributes more to the increase in the modulus. In a nutshell, the replacement of AP with submicron-sized CL-20 provides access to propellants with a higher energy density, but there is an urgent need for the improvement of the processability of the slurries.

At a given CL-20 content of 10%, the GAP propellant slurries containing different gradation ratios of CL-20 were tested. The ratio of submicron-sized CL-20 to micron-sized CL-20 (R) varies from 0.0 to 1.0. Figure 5 displays the storage modulus and loss modulus of the GAP propellant slurries and compares their yield/flow strains. The values of G' and G'', together with the flow strains, follow nonmonotonic trends as R increases. However, the size gradation of CL-20 exerts no significant impact on the initial yield of the GAP slurries.

3.3. Frequency Dependence of the GAP Propellant Slurries. The AP/GAP propellant slurries containing unimodal or bimodal AP were prepared, and subsequently, their rheological properties were acquired by frequency sweep measurements. As depicted in Figure 6, the influence of size gradation of AP particles on the storage modulus (G'), loss modulus (G''), and complex viscosity ($|\eta^*|$) of the AP/GAP propellant slurries is accessible. It should be noted that the rheological parameters of the slurries at 1 rad·s^{-1} are removed as the experimental values present a gross underestimation of the true situation. With an increase in frequency, an opposite trend exists for the values of G' and G'', increasing for G' and decreasing for G''. The structure response of the slurry when sheared over a long period of time can be determined by the rheological properties within the low-frequency regions. In the case of the slurries that are sheared for a long time, the energy stored is reduced while the energy dissipation is increased. During the measurement, the G''-values of the slurries fluctuate more significantly as compared with the G'-values. Furthermore, the values of $|\eta^*|$ decrease with frequency, suggesting the shear-thinning behavior of the slurries, which is in accordance with the results of steady rheological measurements.

On the basis of a 1:1 ratio of ultrafine AP to micron-sized AP, the slurries with 55% AP and 10% CL-20 were tested.

https://doi.org/10.1021/acsomega.2c03872
ACS Omega 2022, 7, 38536−38542

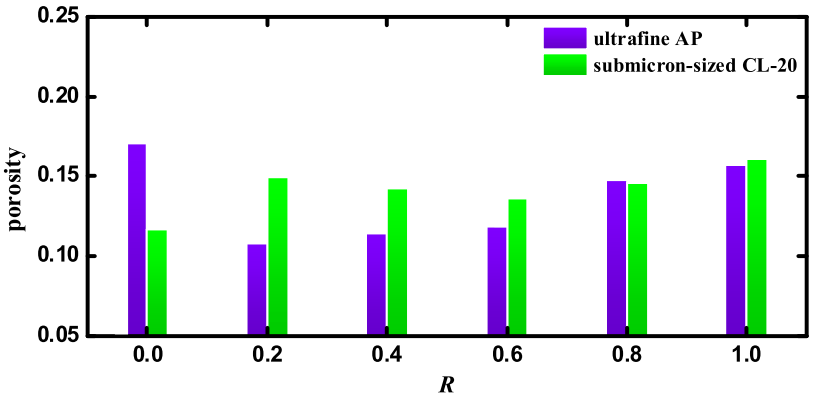

Figure 9. Porosity of loose-packed particles before and after gradation using PFC 2D.

Figure 7 reveals the influence of the size gradation of CL-20 on the storage modulus, loss modulus, and complex viscosity of the CL-20/AP/GAP propellant slurries. As the frequency increases, the values of G' increase and the values of G'' decrease. The characteristics of the reduced storage energy and increased energy dissipation of the slurries are not altered by the introduction of CL-20 when suffering long-term oscillatory shear. Besides, the dependence of G' and G'' on frequency is increased.

The relationship between the relative content of ultrafine AP and submicron-sized CL-20 and the complex viscosity of the propellant slurries was explored, and the results are plotted in Figure 8. The optimum content range of ultrafine AP was found to be approximately 20%, within which the slurries exhibit the lowest viscosity and thus possess the ease of processing. For the slurries with bimodal AP, the $|\eta^*|$-value decreases to a minimum and then increases with an increase in ultrafine AP, the trend of which resembles a parabola. However, the variation of the complex viscosity becomes complicated for the slurries containing both bimodal AP and bimodal CL-20, indicating that insufficient or excessive submicron-sized CL-20 gives rise to the increased viscosity. Fortunately, the appropriate size gradation of CL-20 facilitates the reduction in the viscosity of the slurries despite the addition of CL-20 making the $|\eta^*|$-value increase owing to the reduced particle size. For instance, the $|\eta^*|$-values are effectively reduced to a level that differs inconspicuously from that of the slurries where only AP is included. It follows that the size gradation of CL-20 is a valuable option for promoting the processability of the propellant slurries.

In terms of the CL-20/AP/GAP propellant slurries with a given solid content of 65%, the frictional interaction between particles becomes the main factor influencing the rheological properties, while the thermal motion and the repulsive forces of particles are negligible.[24] When particle gradation technology is applied, potential effects are listed as follows:[10,25] (1) the finer particles with smooth surfaces act as the lubricant at the contact of particles, which can effectively weaken the frictional interactions between particles with sharp edges, and (2) the step-filling effect of micron-sized, ultrafine, and submicron-sized particles contributes to dense packing, resulting in a decrease in the content of liquids trapped in interparticle spaces, which is not conducive to the slurry flow. Hence, an attempt can be made to illustrate and evaluate the differences in the rheological properties of the slurries in terms of factors affecting the interparticle frictional interactions and particle packing density.

PFC 2D, a powerful particle flow code, is of vital application in simulating the interaction of two-dimensional disks with arbitrary geometry and size.[26,27] Treating particles as disks, the loose-packed particles before and after gradation were modeled, and the porosity is illustrated in Figure 9. The porosity of AP particles decreases rapidly for the ultrafine AP's relative content of 0−20%, where AP particles are near the densest packing state. Afterward, the particle porosity increases continually with the relative content of ultrafine AP. The trend of the experimental results on the rheological properties has been captured to some extent. Accordingly, decreasing the particle porosity through optimizing the particle gradation is an economically feasible and practically effective way to prepare suitable propellant slurries with acceptable flowability.

4. CONCLUSIONS

(1) The content of submicron-sized CL-20 exerts little influence on the linear viscoelastic region and the yield transition process of the GAP propellant slurries, as deduced by the mild variations for the yield strain and flow strain ranging from 0.00304 to 0.00483% and 0.0321 to 0.0445% with an increase in the content of submicron-sized CL-20. Moreover, the values of the storage modulus (G') and loss modulus (G'') increase noticeably.

(2) For the GAP propellant slurries containing multimodal particles, the dependence of the storage modulus (G') and loss modulus (G'') on the ratio of submicron-sized CL-20 to micron-sized CL-20 is complex. Moreover, the yield strain is barely altered, while the flow strain changes nonmonotonically.

(3) The values of the complex viscosity ($|\eta^*|$) decrease with increasing frequency, exhibiting shear-thinning. There exists the lowest $|\eta^*|$-value for the slurries after particle gradation when the relative content of submicron-sized CL-20 lies between 50 and 60%. Further evaluation using PFC 2D confirms that the parameter influencing the rheological properties is predominantly the porosity between particles for the GAP propellant slurries.

AUTHOR INFORMATION

Corresponding Authors

Yi Wang − *School of Materials Science and Engineering, North University of China, Taiyuan 030051, China;* orcid.org/0000-0002-9823-6286; Email: wangyi528528@nuc.edu.cn

https://doi.org/10.1021/acsomega.2c03872
ACS Omega 2022, 7, 38536−38542

Xiaolan Song − *School of Environment and Safety Engineering, North University of China, Taiyuan 030051, China;* orcid.org/0000-0001-7870-4874; Email: songxiaolan00@126.com

Authors

Yana Wang − *School of Materials Science and Engineering, North University of China, Taiyuan 030051, China*

Chongwei An − *School of Environment and Safety Engineering, North University of China, Taiyuan 030051, China*

Fengsheng Li − *School of Chemistry and Chemical Engineering, Nanjing University of Science and Technology, Nanjing 210094, China*

Complete contact information is available at: https://pubs.acs.org/10.1021/acsomega.2c03872

Notes

The authors declare no competing financial interest.

■ ACKNOWLEDGMENTS

The work was supported by the Weapons and Equipment Advance Research Fund (No.6140656020201) and the Natural Science Foundation of Jiangsu (BK20211369).

■ REFERENCES

(1) Bumpus, J. A. A theoretical investigation of the ring strain energy, destabilization energy, and heat of formation of CL-20. *Adv. Phys. Chem.* **2012**, *2012*, No. 175146.

(2) Pan, B.; Wei, H.; Jiang, J.; Zong, S.; Lv, P.; Dang, L. Solution-mediated polymorphic transformation of CL-20: An approach to prepare purified form ε particles. *J. Mol. Liq.* **2018**, *265*, 216−225.

(3) Yanju, W.; Jingyu, W.; Chongwei, A.; Hequn, L.; Xiaomu, W.; Binshuo, Y. GAP/CL-20-based compound explosive: a new booster formulation used in a small-sized initiation network. *J. Energ. Mater.* **2017**, *35*, 53−62.

(4) Hussein, A. K.; Zeman, S.; Elbeih, A. Thermo-analytical study of glycidyl azide polymer and its effect on different cyclic nitramines. *Thermochim. Acta* **2018**, *660*, 110−123.

(5) Song, X.; Guo, K.; Wang, Y.; Li, F. Characterization and properties of F2602/GAP/CL-20 energetic fibers with high energy and low sensitivity prepared by the electrospinning method. *ACS Omega* **2020**, *5*, 11106−11114.

(6) Stacer, R. G.; Husband, D. M. Molecular structure of the ideal solid propellant binder. *Propellants, Explos., Pyrotech.* **1991**, *16*, 167−176.

(7) Wang, Y.; Song, X.; Liu, C.; Li, F. Basic property of energetic plasticizer diglycerol tetranitrate (DGTN). *J. Solid Rock. Technol.* **2019**, *42*, 198−204.

(8) Straessler, N.; Lee, M. Synthesis and characterization of diglycerol tetranitrate (DGTN)−an energetic plasticizer for use in explosive and propellant formulations. *J. Energ. Mater.* **2017**, *35*, 1−8.

(9) Park, S.; Choi, S.; Song, J.; Park, E.; Rho, T. A study on the improvement of rheological characteristics of HTPB/AP propellant. *Polym. Korea* **2019**, *43*, 700−704.

(10) Chauhan, D.; Khan, L.; Mandal, S. K.; Jauhari, A.; Bhattacharyya, S. C. Studies on the processing of HTPB-based fast-burning propellant with trimodal oxidiser distribution and its rheological behaviour. *Asia-Pac. J. Chem. Eng.* **2022**, *17*, No. e2783.

(11) Iqbal, M. M.; Raza Ch, S.; Liang, W.; Ali, N.; Raza, A. Investigating the effect of solid fillers on mechanical and rheological properties of composite propellants. *Int. J. Energ. Mater. Chem. Propul.* **2013**, *12*, 75−86.

(12) Cheng, W.; Li, K.; Gao, L.; Feng, C.; An, C.; Ye, B.; Wang, J. Effect of the fractal characteristics of the RDX particles on the rheology of the RDX-based casting aluminized explosives. *J. Energ. Mater.* **2021**, DOI: 10.1080/07370652.2021.2013993.

(13) Guo, X.; Ouyang, G.; Liu, J.; Li, Q.; Wang, L.; Gu, Z.; Li, F. Massive preparation of reduced-sensitivity nano CL-20 and its characterization. *J. Energ. Mater.* **2015**, *33*, 24−33.

(14) Li, F.-s.; Liu, J.; Jiang, W.; Wang, Y.; Guo, X. In *Production and characterization of nanometer explosives*, IEEE 2015 Asian Conference on Defence Technology (ACDT), 2015; pp 23−25.

(15) Rahman, M. M.; Muttakin, M.; Pal, A.; Shafiullah, A. Z.; Saha, B. B. A Statistical approach to determine optimal models for IUPAC-classified adsorption isotherms. *Energies* **2019**, *12*, No. 4565.

(16) Thommes, M. Physisorption of gases, with special reference to the evaluation of surface area and pore size distribution (IUPAC Technical Report). *Chem. Int.* **2016**, *38*, 25.

(17) Sing, K. S. W.; Williams, R. T. Physisorption hysteresis loops and the characterization of nanoporous materials. *Adsorpt. Sci. Technol.* **2004**, *22*, 773−782.

(18) Ramier, J.; Gauthier, C.; Chazeau, L.; Stelandre, L.; Guy, L. Payne effect in silica-filled styrene-butadiene rubber: influence of surface treatment. *J. Polym. Sci., Part B: Polym. Phys.* **2007**, *45*, 286−298.

(19) Shi, X.; Sun, S.; Zhao, A.; Zhang, H.; Zuo, M.; Song, Y.; Zheng, Q. Influence of carbon black on the Payne effect of filled natural rubber compounds. *Compos. Sci. Technol.* **2021**, *203*, No. 108586.

(20) Hyun, K.; Kim, S. H.; Ahn, K. H.; Lee, S. J. Large amplitude oscillatory shear as a way to classify the complex fluids. *J. Non-Newtonian Fluid Mech.* **2002**, *107*, 51−65.

(21) Fan, X.; Xu, H.; Zhang, Q.; Xiao, D.; Song, Y.; Zheng, Q. Insight into the weak strain overshoot of carbon black filled natural rubber. *Polymer* **2019**, *167*, 109−117.

(22) Zhang, X.; Hu, X.; Xu, X.; Zhou, S.; Tang, G.; Pang, A. Surface interaction between GAP binder matrix and ε-CL-20. *J. Energ. Mater.* **2021**, *29*, 1099−1105.

(23) Yin, B.; Su, D.; Lu, G.; Li, Y.; Wu, J. Effect of oxidizers on rheological behavior for GAP based propellant. *J. Solid Rock. Technol.* **2020**, *43*, 566−572.

(24) Wang, B.; Xiong, T.; Gao, L.; Chai, Y.; Cui, X.; Ding, W. Effects of tailings gradation on rheological properties of filling slurry. *Adv. Civ. Eng.* **2019**, *2019*, No. 6873840.

(25) Arefinia, R.; Shojaei, A. On the viscosity of composite suspensions of aluminum and ammonium perchlorate particles dispersed in hydroxyl terminated polybutadiene−New empirical model. *J. Colloid Interface Sci.* **2006**, *299*, 962−971.

(26) Alwaar, A.; Abugharara, A. N.; Butt, S. D. In *PFC-2D Numerical Study of the Influence of Passive Vibration Assisted Rotary Drilling Tool (pVARD) on Drilling Performance Enhancement*, Proceedings of the ASME 2018 37th International Conference on Ocean, Offshore and Arctic Engineering (OMAE 2018), 2018; pp 17−22.

(27) Wu, Z.; Zhang, D.; Wang, S.; Liang, C.; Zhao, D. Dynamic-response characteristics and deformation evolution of loess slopes under seismic loads. *Eng. Geol.* **2020**, *267*, No. 105507.